Monthly Notices
of the
ROYAL ASTRONOMICAL SOCIETY

MNRAS **462,** S23–S32 (2016)
Advance Access publication 2016 August 4

doi:10.1093/mnras/stw1959

Origin of the local structures at the Philae landing site and possible implications on the formation and evolution of 67P/Churyumov–Gerasimenko

F. Poulet,[1]⋆ A. Lucchetti,[2] J.-P. Bibring,[1] J. Carter,[1] B. Gondet,[1] L. Jorda,[3] Y. Langevin,[1] C. Pilorget,[1] C. Capanna[3] and G. Cremonese[2]

[1]*Institut d'Astrophysique Spatiale, CNRS/Univ. Paris Sud, F-91405 Orsay Cedex, France*
[2]*Center of Studies and Activities for Space, CISAS, 'G. Colombo', University of Padova, via Venezia 15, I-35131 Padova, Italy*
[3]*Laboratoire d'Astrophysique de Marseille, UMR 7236, CNRS and Aix-Marseille Université, 38 rue Frédéric Joliot-Curie, F-13388 Marseille Cedex 13, France*

Accepted 2016 August 3. Received 2016 August 1; in original form 2016 June 24

ABSTRACT

In situ images of the 67P/Churyumov–Gerasimenko nucleus acquired by the CIVA cameras on-board PHILAE revealed a rough landscape dominated by consolidated materials. These data provide a unique view to constrain the past and present conditions prevailing at the surface of the comet. A quantitative analysis of microscopic structures (fractures and pebbles) is derived using a manual extraction from the images. Fractures/cracks are rather ubiquitous at various spatial scales with network and size (from sub-cm to 10 cm) well correlated to the texture of the landscape. The pebble size distributions are derived and compared to the size distribution of other cometary materials. The nature of the landscape is then discussed in relation to endogenic and exogenic processes of surface modification. The block seen in CIVA no. 1 is interpreted to be close-ups of fractured boulder/cliff belonging to the boulder field identified from the orbit near Abydos, this boulder field being itself the result of gravitational regressive erosion due to sublimation. The observed fractures are best explained by thermal insolation leading to thermal fatigue and/or to loss of volatile materials. This surficial fragmentation (up to >10 cm length) could generate macroscopic erosion that is also visible at larger scale from the orbit. There is at least an intriguing possibility that the pebbles are remnants of primordial accretion processes. We thus speculate that the Abydos landscape could be in favour of pebble accretion model instead of runaway coagulation model with a formation location in the outer region of the Solar system.

Key words: comets: general.

1 INTRODUCTION

After three touchdowns, Philae came to rest on the surface of the comet 67P/Churyumov–Gerasimenko at the final site Abydos. The lander was equipped with a battery of instruments including the panoramic system of cameras CIVA-P (Bibring et al. 2007) to conduct the detailed characterization of the site and to help operational tasks. The nominal mission started after its separation from Rosetta and lasted $\sim$ 63 h. During this phase, a full panoramic view with CIVA has been acquired. The parameters of this observations and initial investigations have been presented in Bibring et al. (2015). Philae made then several additional contacts with Rosetta during 2015, with the last one coming on July 9 (ESA Rosetta blog). However, these intermittent communications links were too short and unstable to enable any scientific measurement to be commanded. In this paper we thus present additional scientific results associated with the alone panorama performed by CIVA during the nominal operations.

The prime scientific objective of CIVA was to reveal from its imaging capabilities clues about the properties of local structures and the extent to which primordial and/or modern processes were responsible of the cometary nucleus shape. Of special interest for the study of the local morphology of the nucleus are three images, namely CIVA no. 1, no. 3 and no. 4, which revealed a very irregular dust-free landscape, possibly constituting pristine cometary material. Fractures and cracks are observed at different scales, while different textures from relatively smooth surface to pebble agglomerates are observed. These surface characteristics have a unique morphology that defies any easy interpretation. The major objective

⋆ E-mail: francois.poulet@ias.u-psud.fr

of this paper is therefore to map and to quantify some of observed structures and to place constraints on their formation mechanisms through textural characterization and interpretation. After a short reminder of the landing site context observed from orbital and *in situ* observations (Sections 2.1 and 2.2), the textural properties of the two major structures (fractures and pebbles) are evaluated (Sections 2.3 and 2.4). We then speculate on the formation mechanisms that may have sculpted the landscape at the light of the various processes (past and modern) occurring at the surface of a cometary nucleus (Section 3).

2 CONTEXTUAL AND LOCAL STRUCTURE PROPERTIES

2.1 Philae landing site

The landing site has been potentially identified on images acquired by the OSIRIS (Optical, Spectroscopic and Infrared Remote Imaging System) (Keller et al. 2007) imaging system aboard the orbiter before (2014 Oct 22) and after (2014 Dec 6–13) the landing (Lamy et al. 2015). The Philae's location is in the Wosret region, near the boundary of the Hatmehit depression at Cartesian coordinates (2.4491, −0.0703, −0.3554) km in the Cheops reference frame (Preusker et al. 2015; Thomas et al. 2015) (Fig. 1A). The southern hemisphere is dominated by rocky-like, almost dust-free stratified terrains supporting a primordial aspect of this hemisphere in comparison to more dusty northern hemisphere (Lee et al. 2016). As seen from orbit, Abydos is located in an extremely rough dust-free talus with the presence of numerous blocks/boulders (Fig. 1B, Lucchetti et al. 2016). These patterns are typical of the terrains with intermediate gravitational slope (25°–45°), which is exactly the derived value for this talus (Lucchetti et al. 2016). In addition, the Abydos site is characterized by albedo (5 per cent ± 2) and spectral slope (13 per cent/100 nm) that are consistent with the average values of the comet (Lucchetti et al. 2016).

Reconstructions of the local Abydos terrain have been attempted by various teams including the Lander Control Center (LCC DLR Cologne, Jens Biele, private communication), Science Operation and Navigation Center (SONC, Remetean et al. 2016) and OSIRIS science team (Capanna et al. 2015). As the resolution of the available OSIRIS images are low in comparison to CIVA panorama resolution, the use of very specific techniques are required to correlate CIVA images with local OSIRIS-based Digital Terrain Model (DTM). The irregular and complex shape combined to the unfavourable illumination of the Abydos site significantly complicate this comparison. A convincing method called multiresolution photoclinometry by deformation (MPCD) has nevertheless allowed to achieve a good (but not perfect) match between simulated CIVA images from OSIRIS-based DTM and the real CIVA-P panorama (Capanna et al. 2015). A direct comparison between the real CIVA images and the modelled terrain can be found in Jorda et al. (in preparation). The important outcome of this MPCD-based analysis is to confirm the distance of the three major scenes (CIVA no. 1, no. 2 and no. 3) used to quantify the size of local sculptures (Jorda et al., in preparation).

2.2 Geographic distribution of major structures

As stated in the introduction, we focus the analysis on the CIVA no. 1, CIVA no. 3 and CIVA no. 4 images as they provide the most discernible and diverse morphologies of the landing site. The CIVA no. 1 scene is dominated by a fractured block that shadow the

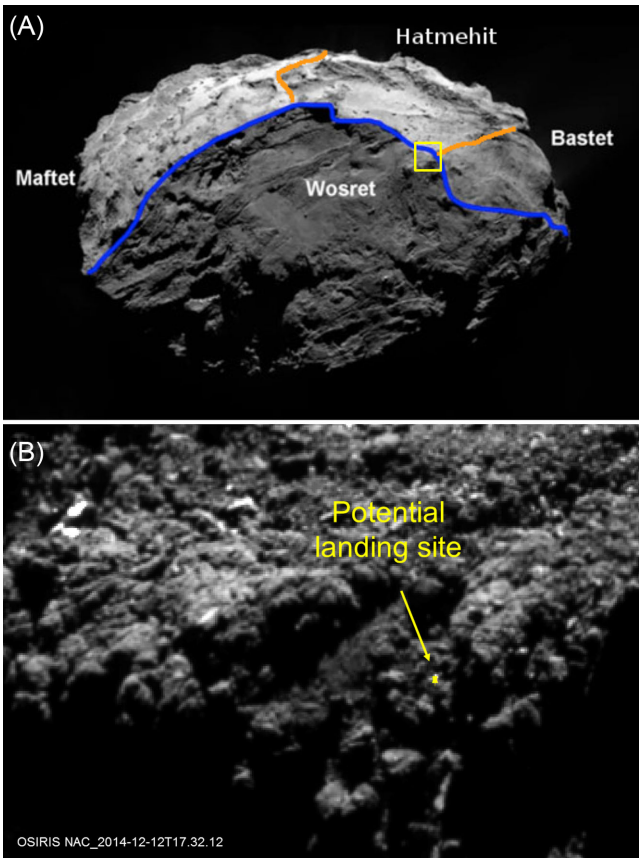

Figure 1. (A) OSIRIS NAC_2015-05-02T10.42.41 image showing the head of 67P/Churyumov–Gerasimenko (Lee et al. 2016) (Credit: ESA/Rosetta/MPS for OSIRIS Team MPS/UPD/LAM/IAA/SSO/INTA/UPM/DASP/IDA). The area of the potential landing site is marked by a yellow square. The Abydos landing site is located in the southern hemisphere at the boundary of the Hatmehit depression and Wosret flat unit. (B) The possible identification of Philae location is symbolized by a yellow symbol (Lamy et al. 2015).

lander (Bibring et al. 2015; Fig. 2). The edges of the block/cliff are backlit by the sun, and the side facing the lander gets some photons from the sunlit foot and leg, suggesting that this structure is rather close to the lander. A rough estimate of the distance based on the lander design is between 1 and 1.5 m, which gives a pixel size in the range 1–1.4 mm (1 mm being taken as a reference below). A first estimate of the distance provided by the MPCD technique is found to be ∼75 +/− 25 cm. Note that, at the time of the writing, there is an on-going campaign by ROSETTA to identify Philae from images acquired at a distance relative to the surface smaller than 5 km. This campaign shall confirm or not the current assumed Abydos position. If it is confirmed, the OSIRIS images will be used to improve the local DTM and therefore the distance of the CIVA no. 1 scene.

CIVA no. 3 and no. 4 reveal a very rugged morphology with large diversity of structures (Bibring et al. 2015). This gives a rocky appearance, although it is important to recognize that the bulk density of the material is probably 5 times or so lower than the densities of terrestrial silicates. A major characteristics of the landscape is also the absence of dust or sand-like mantle in contrast to the Agilkia site where a regolith layer was observed by ROLIS (Rosetta Lander Imaging System) with a thickness varying from 1 to 2 m (Mottola et al. 2015). Information on the spatial resolution of the

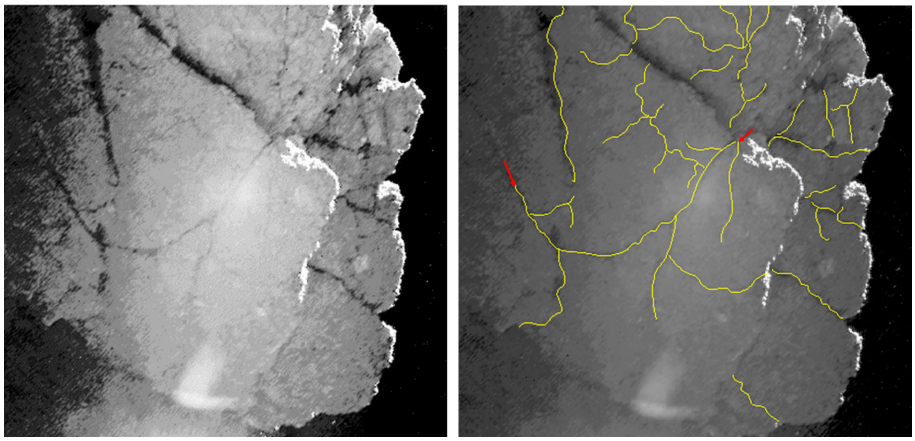

Figure 2. Close-up from CIVA no. 1 showing the fractured block. The left image was stretched to emphasize the fractures. The two reds arrow indicate the limit of the fracture having the maximum length (537.6 mm at 1 mm pix^{-1} resolution or 752.6 mm at 1.4 mm pix^{-1} resolution).

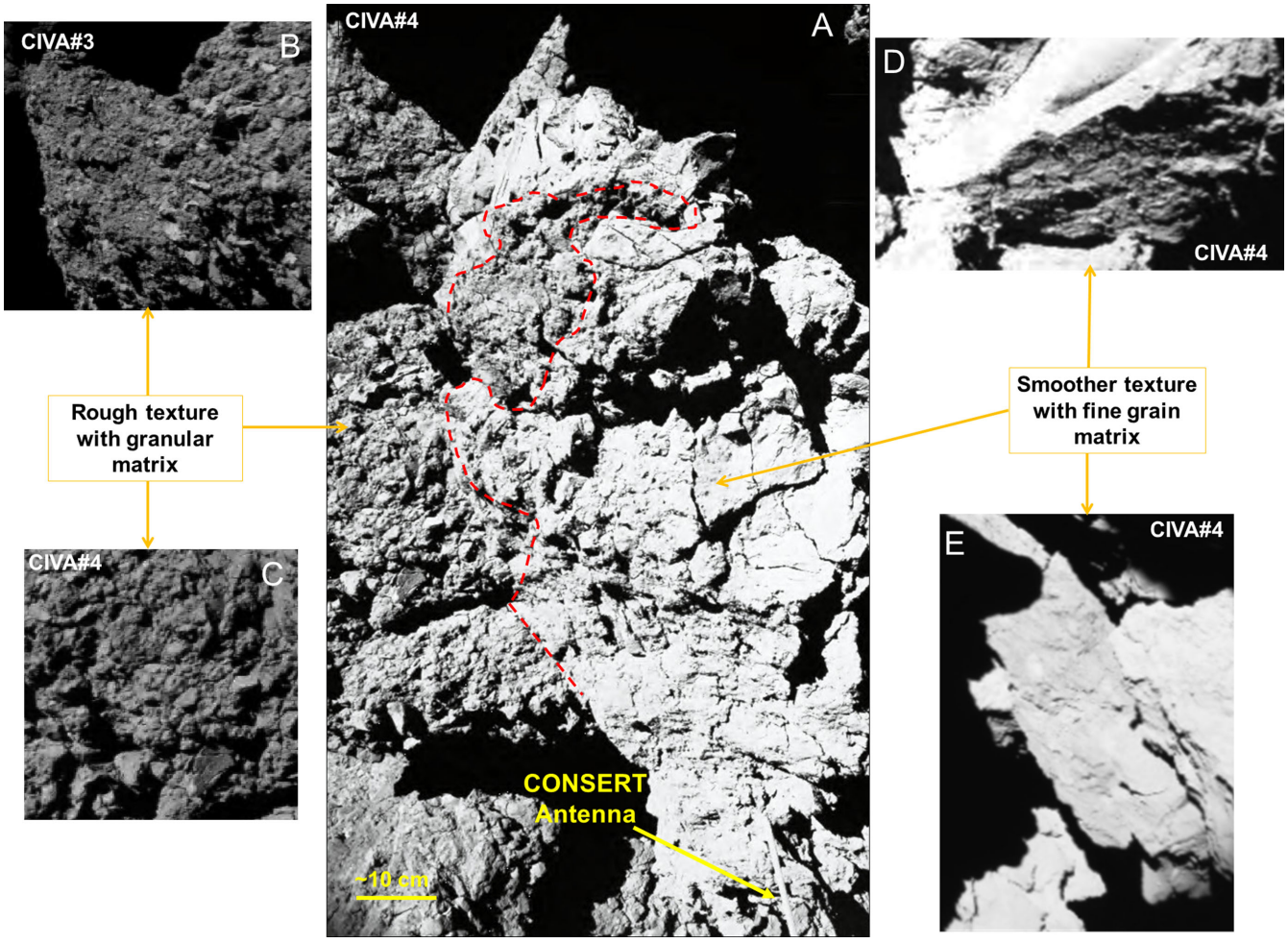

Figure 3. Close-ups of CIVA no. 3 and CIVA no. 4 exhibiting the two major types of texture. The contact between the two units is emphasized by the dashed red line on (A). Granular texture is visible on (B) and (C), a smoother texture is seen on the right part of CIVA no. 4 (close-ups D and E).

two images can be obtained by the +X foot of Philae and the CONSERT antenna. This gives a resolution of 0.91 mm pix^{-1} and 0.625 mm pix^{-1} for CIVA no. 3 and CIVA no. 4 images, respectively if all structures are assumed to be in the same plan (which is likely not the case, see Section 2.4). As exemplified in Fig. 3, variations in texture and albedo are observed in these images: a unit of low albedo with irregular surface interpreted as a rough texture looks visible on CIVA no. 3 (Figs 3B and C) and on the left part of CIVA no. 4 (Fig. 3A), while brighter (sometimes saturated) and smoother texture is found on the right part of CIVA no. 4 (Figs 3A, D and E). The rough texture unit appears to be granular with spatially resolved grains (called pebbles), while the smoother

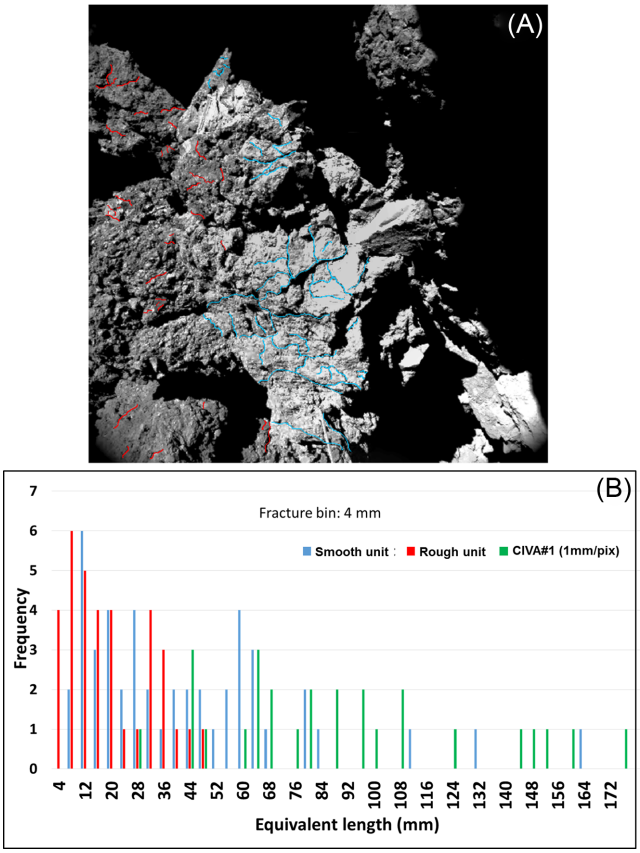

Figure 4. (A) Map of the fractures on CIVA no. 4. The fractures observed in the smooth (resp. rough/granular) unit are in blue (resp. red). (B) Histogram of frequency versus fracture lengths of the three major lithologies. The fractures referred as to CIVA no. 1 (green bars) are mapped on Fig. 2. The bin size is 4 mm, which corresponds to the smallest fracture found on images and to a value larger than three pixel sampling, which minimizes the likelihood of misidentifications (Nyquist 1928).

unit seems to contain a fine-grain matrix as revealed by a remaining irregular outcrop interpreted to be the result of a lithic fragmentation (Fig. 3D). The contact between the two types of texture is visible at the centre of CIVA no. 4 field of views (Fig. 3A), indicating a pretty clear discontinuity. In the upper part, the rough unit looks to sit uncomfortably on the smooth unit, but such stratigraphy is much less obvious in the lower part.

2.3 Fractures

Fractures are preferentially observed on CIVA no. 1 (Fig. 2) and CIVA no. 4 (Fig. 4). A systematic mapping of these structures was performed using manual identification. Specifically, the mapping was carried out with ARCGIS software, identifying the fractures as polylines and, hence, calculating their equivalent length. We have counted 34 fractures in CIVA no. 1 image and 82 in CIVA no. 4. In CIVA no. 4, two different classes of fracture were considered by separating fractures belonging to the smooth texture unit (47 fractures in total) from those belonging to the rough unit (35 in total).

The fracture mappings are shown on Figs 1 and 4A. In the cases of the boulder (yellow lines on Fig. 1) and the smooth unit (blue lines on Fig. 4A), they form poorly developed networks without forming any polygonal shape in contrary to the well-developed and common networks visible from the orbit (El Maarry et al. 2015). The block on CIVA no. 1 presents the most complex network and the longest fractures (up to 10 s of cm with an average of 128 mm using the 1 mm pix^{-1}). The fractures are rather linear and not conchoidal. Their overall morphology suggests than the fragmentation is initiated from a mechanical weakness (e.g. microscopic crack) and then propagated and extended slowly, until some junction occurs. Such a typology seems to be indicative of a slowly evolving stressed system.

The fractures on the rough/granular unit (red lines on Fig. 4) are much smaller, isolated and do not form any network. Although we cannot exclude the presence of intragranular cracks (cracks that lie within the grain) due to the limitation on the spatial resolution, the resolved fractures extend outside the resolved grains, possibly within cemented material between grains. The histogram fracture length shows that the majority of the fractures of the rough unit is smaller than 50 mm (Fig. 4B). Their length is in average smaller than that of the smooth unit (22 mm versus 45 mm).This implies that the texture (itself related to the lithology) likely controls the surficial fragmentation. The fact that the formation mechanism is driven by the mechanical properties of the material is also consistent with the absence of fractures on CIVA no. 3 whose scene is dominated by pebble agglomerate (see Section 2.4).

The angles of intersection are variables, but not well defined due to the lack of 3D information that could potentially imply significant uncertainty on the fracture directions (and thus propagating error on the angles). We however attempt to measure the mean angles of separation between fractures for some parts of the data set. Angles between 30° and 80° are found for fractures of CIVA no. 1 and between 40° and 70° for fractures belonging to the smooth unit of CIVA no. 4. The fractures identified on the rough unit were excluded from the statistics since they are not a well-developed fractures network. This information could be potentially valuable for modeller.

2.4 Pebbles

A large part of the landscape is covered by a consolidated granular material with complex and irregular shape. A survey of this granular material could classify this peculiar texture into two classes: (1) 'pebbles' as resolved grains of size larger than a few CIVA pixels; (2) 'unresolved grains' as rough material that is present between the pebbles. This last class cannot be studied as a textural class because of their size lower than the CIVA detection limit. For the pebble class, a systematic mapping was performed using visual identification. The pebbles detection has been performed with the same technique used for cometary boulder counting (Pajola et al. 2015, 2016). Hence, we defined as pebble a positive relief with the presence of elongated shadow, whose extension depends on the illumination geometry. These features were manually identified and extracted with the software ARCGIS. Assuming their shapes as polygons, we derived their maximum length that is the equivalent diameter and their corresponding area. Only pebbles larger than six pixels were identified, which minimizes the likelihood of misidentification. We have counted 283 and 412 pebbles on CIVA no. 3 and CIVA no. 4 images, respectively.

A limitation coming from two-dimensional imagery is the accurate knowledge on the distance for each CIVA pixel, which can be extrapolated only from spatial reference, Philae foot for CIVA no. 3 and CONSERT antenna for CIVA4 (Bibring et al. 2015). As no definitive and accurate local DTM of the site has been so far derived, we thus decide to restrict the conversion in cm to the pebble size located on the forefront of each image, for which the spatial resolution

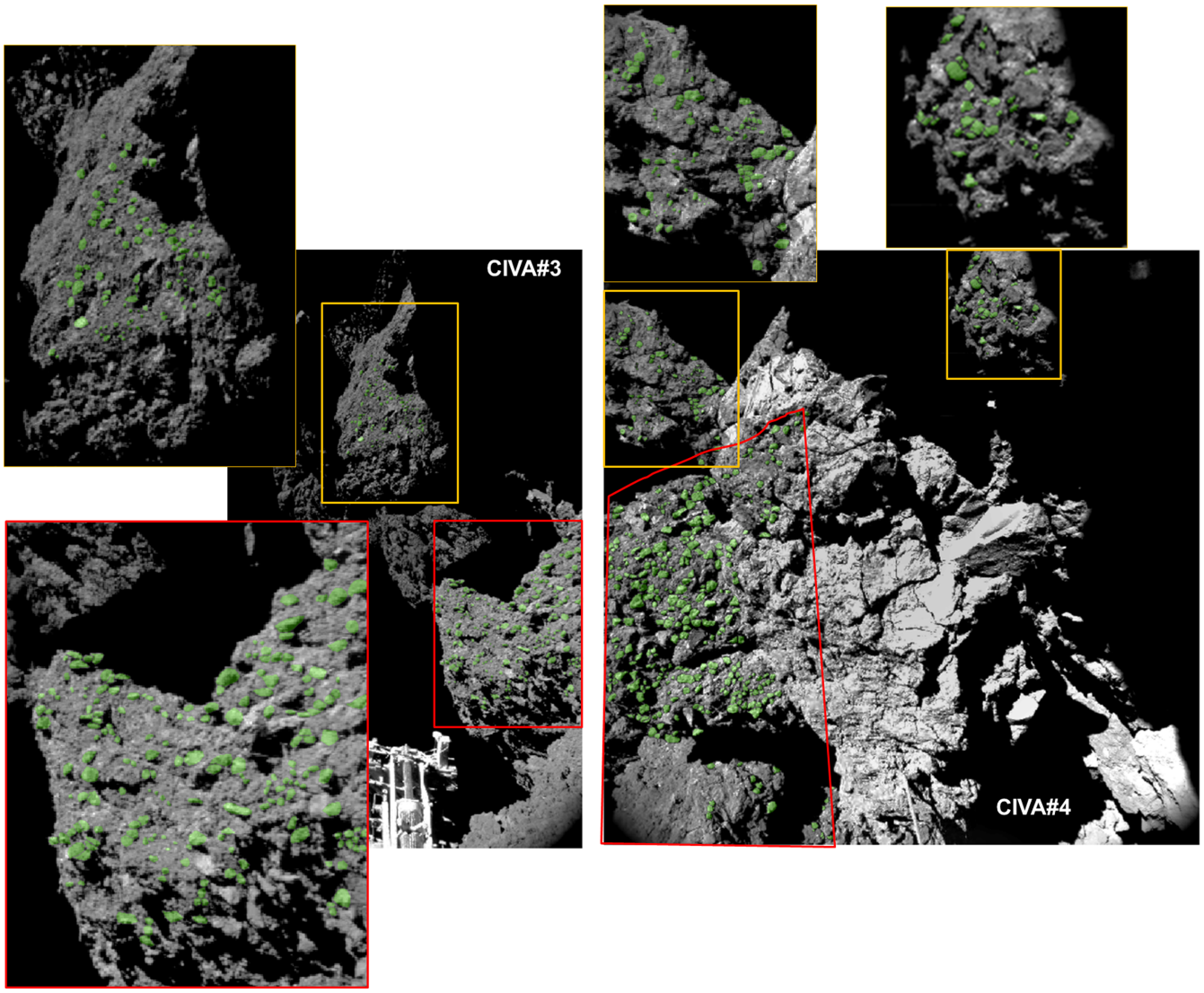

Figure 5. Map of pebbles (in green) for CIVA no. 3 and no. 4. Orange and red boxes show the locations of the highlighted areas. Only the pebbles inside the two areas delimited by the red lines were used for statistical purpose (see text).

is the best known. These two forefronts are defined by red lines on Fig. 5. Measured pebble size varies from 3.7 to 16.25 mm. We then examine the cumulative pebble size-distribution of the two regions (Fig. 6). The fact to add the number of pebbles with reliable size of the two CIVA images has the advantage to improve the statistics. The pebble population significantly decreases for sizes larger than 12 mm, while the number of small pebbles (<5 mm) reaches a plateau partly due to the CIVA spatial resolution (∼1 mm). Three distinct power laws are required to fit the data with index values of −0.37 for the smallest pebbles (3–5 mm), −2.9 for intermediate-sized pebbles ranged in the 5–11 mm and $-11.8 + 2/-2.8$ for the largest pebble sample. The large power-law index value can be partly due the poor number of pebbles of size >1 cm as indicated by the large error bar as indicated by the large error bar of this parameter.

The fact that a unique power law cannot well explain the pebbles size frequency distribution is reinforced by additional analysis of pebbles located in the orange boxes outlined in Fig. 5. For each orange box, pebbles cumulative size–frequency distribution was calculated by keeping the pebble size in pixel to avoid the introduction of uncertainties due to the conversion in mm. Depending on the statistics of the pebble population, we found that at least two different power-law indexes were required to fit their distribution behaviour.

4 POSSIBLE FORMATION PROCESSES

A number of plausible hypotheses can be proposed to explain the extra-terrestrial landscape of Abydos. Although the material could be primordial as suggested by Lucchetti et al. (2016), present modern processes have possibly participated in the reshaping of the surface. One of the key questions is whether all the small-scale sculptures can be only the result of thermal insolation (inducing mainly ice sublimation and thermal fatigue followed by erosion and reshaping by gravitational slope) as it is suggested for large-scale morphology observed from the ROSETTA spacecraft (e.g. Thomas et al. 2015). An additional panorama could have to tackle this problem by checking any surface change with time. As one and only one panorama was acquired, we thus assess a variety of explanations including exogenic/endogenic/modern/past ones.

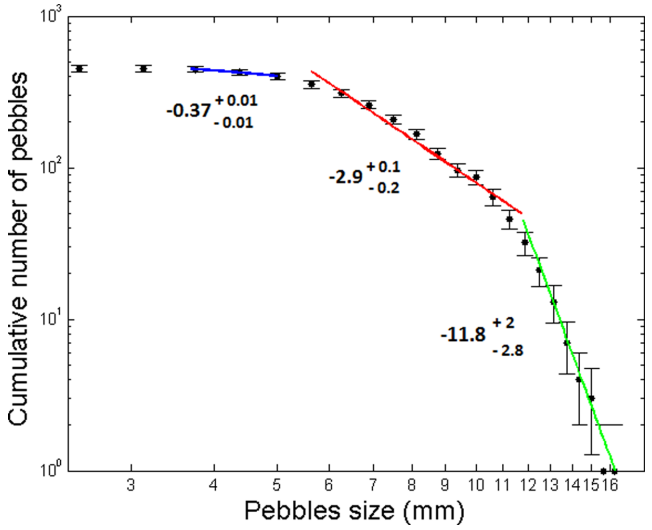

Figure 6. Cumulative size–frequency distribution of pebbles larger than 3.7 mm (6 CIVA pixels) identified on the two forefronts of the CIVA no. 3 and CIVA no. 4 images (see Fig. 5 for delimited areas). The bin size is 0.625 mm and the vertical error bars indicate the root of the cumulative number of counting pebbles (as from Michikami et al. 2008). The fitting regression lines give a power-law index of $-0.37 + 0.01/-0.01$,$-2.9 + 0.1/-0.2$ and $-11.8 + 2/-2.8$ for size ranges between 3.7–5.6 mm, 5.6–11 mm and 11.8–16.2 mm, respectively.

4.1 Exogenic processes

Before being ejected into its current orbit, the nucleus as other small atmosphereless bodies has undergone exogenic processes. Among them, we can mention high energy particles and solar wind bombardment, micrometeoritic bombardment, and impact cratering events. Given the lack of fine particle blanket at the landing site, there is no evidence of a long term and continuous battering by micrometeoritic bombardment. High energy particles and solar wind bombardment is expected to induce the formation of a brittle crust that is not observed on CIVA images. Such loosely bound crust is also not really supported by MUPUS (Multipurpose Sensors for Surface and Sub-Surface Science) measurements of the thermal inertia and the strength of several MPa since the instrument was not able to penetrate the surface material below a few centimetres (Spohn et al. 2015). A thin layer of dust may be present but it is speculative according to Spohn et al. (2015) and not visible at CIVA resolution.

The collisional (and gravitational re-accumulation) processes could lead to the creation of a rugged and complex landscape. For a comet, collisions could have occurred following its formation in the trans-Neptunian primordial disc or within the scattered disc, so that most of km-sized Jupiter Family Comets (JFC) such as 67P are interpreted to be collisional fragments (Davis & Farinella 1997; Morbidelli & Rickman 2015). On the other hand, Davidsson et al. (2015) proposed that 67P was formed in a dynamically cold primordial disc preserving the nucleus as a primordial body. This primordial aspect is also supported by the presence of stratification as a dominant structural aspect of 67P (Massironi et al. 2015). In any case, it is out of scope of the paper to discuss these two concurrent models at the light of the CIVA panorama, so that we cannot conclude on the primordial collisional hypothesis.

After the injection into its current short period orbit for several millions, the surface of the cometary nucleus can be impacted by projectiles of various origins inducing crater impacting events. This can be a small asteroidal object or fragments of the cometary nucleus from other or the same comet (Ivanova et al. 2015). These fragments can be tiny meteoroids but also macroscopic bodies as m-sized particles have been already detected in the close environment of comets including 67P (A'Hearn et al. 2011; Rotundi et al. 2015). In addition to impact structure, repetitive non-destructive impacts could produce size sorting due to the seismic shaking (Matsumura et al. 2014; Tancredi et al. 2015). Craters were observed on the surfaces of comets 9P/Tempel 1 and 81P/Wild 2 with sizes significantly large (up to 1 km) to be the result of 10-m impactors (Ivanova et al. 2015). Conversely, the surface of 67P is almost devoid of recognizable impact craters (Thomas et al. 2015). Current collision rates for comets are also expected to be very low (Vincent et al. 2015a) making the impact mechanism very unlikely to trigger the formation of Abydos landscape. This view is supported by the 67P boulders analysis performed by Pajola et al. (2015a) who discard an impact origin of the formation of the boulders observed by OSIRIS. On the other hand, Philae is at the proximity of the Hatmehit circular depression, whose impact origin cannot be totally excluded (Pajola et al. 2015a; Thomas et al. 2015). The two units observed by Philae have an unconformable contact, suggesting a mechanism leading to an overlap of materials. We could thus speculate that this overlapping swirl of materials was the result of impact. However, as mentioned by Thomas et al. (2015), the details of the creation of the rim and of the final distribution of fluidized ejecta at any spatial scale is totally unknown to date, which defies any easy conclusion on the involvement or not of the impact cratering event into the formation of the Abydos landscape.

4.2 Endogenic modern processes

Possible endogenic modern processes put forward by the literature to explain the surface structures of 67P are (i) *erosion by sublimation* that could create collapse, depression and gravitational events; (ii) *fragmentation* through loss of volatile materials (e.g., desiccation), thermal fatigue or tectonic processes; (iii) *recondensation* and/or *sintering* that uniform the near-surface by producing a vertical stratification (with an uppermost porous mantle of refractory dust overlaying a layer of hard ice); formation of lag deposit by (iv) *redeposition* of particles due to cometary activities; (v) *size segregation* (Brazil Nut Effect) due to shaking; (vi) *fluidization and multiphase transport* of cometary material related to outbursts. In the following, we review each of these processes to evaluate whether they are involved in the formation of Abydos.

To explain the MUPUS measurement, the presence of a hard layer of water ice near the surface was postulated (Spohn et al. 2015). It could be the result of sintering or recondensation of the water ice leading to the segregation of the ice and dust components, with eventually the formation of a thick layer of hard ice below the uppermost dust layer of low albedo. This process occurs at cometary scale and is a convincing explanation of the uniform low albedo of the comet (Pommerol et al. 2015 and references therein). If this process was dominant at Abydos, the presence of a dust layer should be visible and makes uniform the scene at cm-scale. However, significant albedo variations (3–10 per cent) are observed in the scene of CIVA (Bibring et al. 2015). Unless the uppermost layer of organic/mineral dust is very thin (a few mm at most), the cm-scale morphology detected by CIVA does not reveal any presence of a dust layer that could smooth the texture. Therefore, we consider that the cm-scale morphological structures visible on the CIVA panorama are not due to a vertical stratification from sintering/recondensation process (process numerated iii).

We found no obvious evidence of dust remobilization and formation of lag deposit by cometary activities (process iv). The only hint of redeposition could correspond to a few loosely bound grains on the background of CIVA no. 3 (Bibring et al. 2015). We attempted to overlap the gravity field on the local shape model, but the uncertainties on the different models preclude to have any estimate on the gravitational slope of the cliff where these grains are located. Size segregation due to shaking (process v) was proposed to explain the size distribution of individual structures of various sizes on asteroids (Matsumura et al. 2014; Tancredi et al. 2015). The shaking could be triggered by cometary scale thermal variations, impact or collapse due to erosion. No evaluation of this mechanism on the boulder distribution has been performed (Pajola et al. 2015), but there are several pieces of evidence that other processes can well explain the boulder distribution on 67P. Therefore, we consider that this mechanism is little plausible to explain any feature observed by CIVA.

On cometary nuclei, the removal of subsurface volatiles is expected to generate a void (process referred as to i and discussed later). Meanwhile, materials erupting from the interior of the comet could create specific features on the surface (process vi). The most prominent feature due to this process is km-scale smooth regions detected on 81P/Wild 2, whose topography is consistent with flows and ponded regions (Thomas et al. 2007; Cheng et al. 2013). Belton & Melosh (2009) came up with a fluidization mechanism to explain this structure. It consists of an outflowing vapour through a granular medium lifting and separating the grains, so that the medium can flow like a fluid. During the acceleration of the flow, a grain size separation between large and small particles could occur leading to a difference in texture and albedo. We could thus argue that the fluidization process is the best explanation for the juxtaposition of two textures observed on CIVA images. Specific conditions are nevertheless required for fluidization, which have apparently not be met on all comets including 67P as demonstrated by the absence of smooth regions. Outburts from 67P have well been observed as earlier than 2014 April. Most of the first activity events came out of a very specific area, the transition region between the small and large lobes of the nucleus (called the Hapi region, Sierks et al. 2015). OSIRIS then followed the activity from 2014 August to 2015 May, revealing an activity restricted in the northern hemisphere and correlated to rough and fractured cliffs as well as pits (Vincent et al. 2015b, 2016). Although active sources were mapped in the head, no activity was reported near Abydos. Moreover, the primary effect of this activity on the surface evolution is erosion and not fluidization (Vincent et al. 2016). Although we cannot totally exclude that fluidization could occur at small scale level, we consider that the diverse comet surface textures as observed by CIVA can be hardly explained by any known process.

On the contrary, the origin of the block observed on CIVA no. 1 looks less enigmatic. As described in Lucchetti et al. (2016), Philae is very close to a well-defined unit, namely a talus mainly made of fallen consolidated materials and debris fields, with numerous boulders from <1 m to 10 m. We therefore attribute the origin of the block seen in CIVA no. 1 to this debris field. The talus with intermediate gravitational slope is a typical example where the morphology appears well controlled by the gravitational slope as also observed in numerous terrains (Groussin et al. 2015).

Most of the fractures observed at large scale from the orbit are interpreted to be driven by tensile stresses, resulting from short-term thermal shock or long-term thermal fatigue (El Maarry et al. 2015). Sublimation-driven desiccation is also evoked although less frequent. It is thus tantalizing to explain the fractures observed at smaller scale by CIVA by the same mechanisms (process ii). Two sets of observations support this view. First, the Abydos site is in a region surrounded by layered and fractured outcrops and a talus deposit rich in boulders, whose size distribution is best explained with gravitational events triggered by sublimation and/or thermal fracturing causing regressive erosion (Lucchetti et al. 2016). Secondly, the morphology of the boulder on CIVA no. 1 looks similar to that of boulders seen at high spatial resolution by OSIRIS and ROLIS, i.e. having fractured structure with decimetre-scale rounded knobs (El Maarry et al. 2015; Mottola et al. 2015; Pajola et al. 2015). The fractures play a role in the shape of these boulders by fragmentation as it is also suggested for the block of CIVA no. 1 image. Detailed modelling of thermal fatigue would obviously help to confirm or not that this mechanism is responsible for the observed fractures from cm- to 10-cm scales. A study has been already performed for the asteroids (Delbo et al. 2014), but investigation for cometary material of uncertain composition and in a not-well defined thermal context requires modelling in a parameter regime not yet explored. Note also that these simulations shall be able to reproduce the difference between the fractures of the smooth unit and those of the granular unit (Section 2.3). In granular rocks, grain size influences strength. For constant porosity and composition, a smaller grain size means greater strength. This tendency can be understood in terms of grain contact models (Eberhardt et al. 1999). If all the observed fractures were the results of thermal fatigue, we would expect larger fractures for granular unit than for the smooth unit. The observations are opposite to this prediction, which could suggest either different composition or porosity or that another mechanism such as sublimation-driven desiccation was involved into the fracture formation.

We now question the origin of the pebbles by exploring whether the pebbles could the result of recent processes. The presence of domains with different size distributions could suggest the existence of mechanisms for particle size evolution, sorting, and/or transport. We thus compare their size distribution derived in Section 2.4 with size distributions of cometary materials coming from a variety of sources and modern processes (Table 1). In other term, can we explain the size distribution of the pebbles by similar recent processes that sculpted the regolith of Agilkia site, the global and local boulders distribution, as well as grains ejected by the cometary activities? The fits of the size distributions of other cometary materials require only one or two regime instead of three for the pebbles. For larger-than-millimetre sizes, the same size distribution at the nucleus surface is inferred by direct pebble counts on the nucleus smooth terrains (ROLIS), by single particle detections inside the dust coma (OSIRIS + GIADA) and by coma-tail-trail models applied to ground based observations (Agarwal et al. 2010). Hence, grain does not change its size during all its days-long travel in 67P coma. The boulders have more complex size distributions interpreted to be the result of various physical processes (Table 1). However, their power-index values are significantly different from those obtained at the landing site. It is thus difficult to reconcile the pebble size distribution with the recent processes that on one hand formed the regolith observed by ROLIS and on the other hand sculpted the boulders in different areas of the comet including the boulder field very near the landing site (Lucchetti et al. 2016). This result hints at a different origin of the observed pebbles.

The comet activity is associated with the liberation of particles from its surface by the sublimation of the abundant volatile ices. We then investigate whether a size segregation produced by these activities could explain the observed pebble population (size in the mm-cm range). MUPUS indicates strengths far larger than typical

Table 1. Compilation of the power-law indexes derived for the size distributions of pebbles observed in CIVA images and of individual fragments (regolith particles, boulders, coma particles) observed in the close environment of the comet 67P by various instruments.

Region of interest (dataset)	Size range (cm)	Power-index and interpretation	Reference
Pebbles at Philae landing site (CIVA no. 3 and no. 4)	1.1–1.6	−11.8	This work
	0.55–1.1	−2.9	
	0.3–0.55	−0.7	
Regolith particles at Agalkia site (ROLIS images)	Smooth terrains: >4	−2.8 +/− 0.2 Mantling deposits due to particles falling back on 67P surface	Mottola et al. (2015)
	Rough terrains: 4–40	−2.2 +/− 0.1 −3.5 +/− 0.3	
	>40	Lag deposits	
Boulders at Agalkia site (OSIRIS image)	>2 m	−3.2 to −2.8 Smooth fine deposits and gravitational accumulation deposits	La Forgia et al. (2015)
Outflowing grains in the 67P coma between 3.6 and 3.4 au (GIADA and OSIRIS)	<0.1	−1	Rotundi et al. (2015)
	>0.1	−3	
Collected dust grains (COSIMA)	10 s μm to mm	−2.1	Hilchenbach et al. (2016)
Boulders on the talus near the landing site (OSIRIS)	100–1160	−3.7 to −4.4 Gravitational events triggered by regressive erosion	Lucchetti et al. (2016)
Boulders on 67P (OSIRIS)	>7 m	−6.5 to −5 Collapse/pit formation and creation of depressions	Pajola et al. (2016)
	>7 m	−4 to −3.5 Gravitational events from regressive erosion	
	>7 m	−2 to −1 Sublimation only	

gas pressures caused by the sublimation of the ices (Spohn et al. 2015). This would imply that the dust grains cannot be currently detached from the surface seen by Philae by the gas pressure of the sublimating ices. However, the production rate implies complex process such as material structure (e.g., cohesion of the material as a function of porosity and packing structure) and physical properties (e.g., heat conductivity, rate of outflowing gas molecules). We thus assume that the conditions at the Philae landing site were different in the past, allowing ejection of material by ice sublimation. Assuming that the nucleus consists of dust aggregates, Gundlach et al. (2015) calculate the size range of the dust aggregates able to escape from the nucleus by the outgassing of icy materials as a function of the heliocentric distance. They found that the most likely particle to escape has a size of ∼1 dm. The size range of ejected particles widens with decreasing heliocentric distance, and except for μm-sized monomer grains, almost all larger grains (up to m-sized) can be detached from the surface. This model is not really consistent with the strong depletion of larger cm-sized pebbles if it was the result of size segregation by the dust activity. Note that a large range of sizes (from 10 s μm to m) has been identified during the pre-perihelion phase (Rotundi et al. 2015). Mottola et al. (2015) also remark that the size distribution for cm-sized particles calculated in the smooth terrains of Agilkia is similar to the one estimated for outbound largest particles. This suggests that the observed size distribution of the largest outbound particles is the same as the size distribution at launch. In summary, both modelling and observations point out that the current cometary activity is not involved in the explanation of the pebble population.

4.3 Relationship between pebbles and accretion processes

As a recent origin of the pebbles remains somewhat unlikely, it is thus possible that they are related to the earliest stages of the formation of the comet. The hypothesis that Philae is located on a primordial terrain is actually supported by the morphological analysis of the Abydos region (Lucchetti et al. 2016). Overall, the primordial nature of the nucleus is also supported by the presence of stratification as a dominant structural aspect of 67P. As explained in Massironi et al. (2015), the comet stratification shows that the two lobes are the expression of two separate objects, maybe formed as pebble-pile planetesimals that are evidently characterized by onion-like stratification several hundred metres thick. Last

decade advancements in planet formation theory suggest that the initial cometestimals (and planetsimals) grow directly from the gravitational collapse of aerodynamically concentrated small particles, often referred to as 'pebbles' (e.g., Youdin & Goodman 2005; Johansen et al. 2007, 2009; Wahlberg Jansson & Johansen 2014). Assuming the cliff preserves a physical record of the primordial accretion (original cometesimals of 67P/GC or larger planetesimals), we here discuss that the observed pebbles may be indicative of the particles from which the initial cometary bodies formed.

There are basically two standard planetesimal accretion models, the hierarchical growth one and the pebbles accretion one. Both assume dust grains (μm) collide and stick together to form cm-sized bodies (and even larger for the coagulation one). Divergence after this first step occurs. In the hierarchical model, contact forces during collision lead to sticking and forming large building blocks, with km-sized comets made from binary collisions of building blocks of sizes in a narrow range of 10 –100 s of metres (Weidenschilling 1997). Larger Kuiper belt objects are also formed by accretion of these small "cometesimals" (Kenyon & Bromley 2004). In the other model, pebbles can clump together through the streaming instability, form gravitationally bound pebble clouds that will collapse according different regimes depending on the mass of the cloud (Wahlberg Jansson & Johansen 2014). It may then form objects as large as 10^2 to 10^3 km or as small as the 67P nucleus.

The presence of pebble agglomerates as revealed by the CIVA panorama agrees with the idea of 67P being piles of mm and cm-sized pebbles and may hint a primordial origin of the pebbles. The pebbles mass fraction depends on the initial mass in the cloud from which the comet was formed (Wahlberg Jansson & Johansen 2014). For 67P, the accretion model predicts that the nucleus of 67P should be a pebble-pile planetesimal consisting of primordial pebbles (from mm to cm-sized) assuming the nucleus is the result of a low mass vortice. In the case of higher initial mass cloud leading to planetesimals larger than 10 km, they collapse with fragmentation decreasing the pebble mass fraction, and the resulting planetesimals therefore become mixture of pebbles and dust with a high density (Wahlberg Jansson & Johansen 2014). The low density of 67P (532 ± 7 kg m^{-3}, Jorda et al. 2016) would be thus more consistent with the collapse of a low mass pebble cloud. On the other hand, 67P objects could also form later as individual or reaccreted fragments produced by collisions of large objects, but such a scenario is not supported by several observational facts (Davidsson et al. 2015) including layering up to 650 m deep (Massironi et al. 2015). Another hint in favour of the pebble accretion model comes from the low value for the tensile strength comparable to that of dust aggregates formed by gravitational instability consistent with accretion of pebbles at low velocities (Groussin et al. 2015). Note however that the relation between the observed pebble size distributions and the processes of pebble accretion is still unknown.

It is also interesting to see if we can predict the formation location of the comet from the observed pebble sizes. Kretke & Levison (2015) evaluates the size of pebbles as a function of heliocentric distance for a normal protoplanetary disc under different hypotheses. If the pebble size range observed by CIVA turns out to be representative of the nucleus, it would indicate a formation occurring under low value of the Stokes number ($<10^{-1}$) and preferentially in the outer regions of the Solar system (distance >5 to 20 au depending on the initial conditions of the model). This is consistent with the high D/H ratio (Altwegg et al. 2015) and the N2/CO ratio (Rubin et al. 2015) indicating that 67P formed in the colder-outer regions of the Solar system.

5 CONCLUSION

The Philae lander measurements coupled to the Rosetta observations transformed the comet 67P (Churyumov–Gerasimenko) from an astronomical object into a geological object with a variety of complex structures. Based on the analysis of CIVA images, we investigated the different physical processes that may have sculpted the various local landforms observed at the Philae landing site. A quantitative analysis of grains that look like pebbles and fractures was derived. We conclude that some endogenic modern processes can likely explain some features revealed by CIVA. Specifically, the fragmentation by thermal insolation and/or loss of volatiles is the most plausible mechanism for creating the observed fractures. These fractures could trigger surface evolution and long-term erosion at cm-scale as also commonly observed at larger scale from orbit. The block seen in CIVA no. 1 is probably a close-up of a fractured boulder belonging to the boulder field present on the talus surrounding the landing site. A difference of texture is observed in CIVA no. 3 and no. 4 and tentatively explained by impact cratering and sublimation-driven fluidization. However, none of these two mechanisms provides satisfactory explanation so that the formation remains unknown. Further modelling of impact cratering, sublimation, accretion and fragmentation processes at very small spatial scales (from metre to centimetre!) could perhaps help to better constrain this surface feature. While we cannot conclusively state that the resolved particles are primordial, these pebble population is difficult to be explained by any modern process. Assuming the pebbles observed by CIVA are remnants of the gravitational collapse of pebble swarms created by streaming instabilities, their size indicates a formation location in the outer regions of the Solar system (minimal heliocentric distance >5–20 au according to accretion models) under low values of the Stokes number.

ACKNOWLEDGEMENTS

The authors thank the SONC (Science Operation and Navigation Center, CNES Toulouse), the Rosetta Mission Operations Centre at ESOC and the Lander Control Center at DLR Cologne for their outstanding work enabling the science return of the Rosetta/Philae missions. FP wishes to thank J. Biele (DLR), M. Delbo (Observatoire de Nice) and S. Charnoz (Université Paris 7) for fruitful discussions.

REFERENCES

Agarwal J. et al., 2010, Icarus, 207, 992
A'Hearn M. F. et al., 2011, Science, 332, 1396
Altwegg K. et al., 2015, Science, 347, 3
Belton M. J. S., Melosh J., 2009, Icarus, 200, 280
Bibring J.-P. et al., 2007, Space Sci. Rev., 128, 397
Bibring J.-P. et al., 2015, Science, 349, 6247
Capanna C. et al., 2015, DPS meeting 47, Abstract 413. p. 11
Cheng A. F., Lisse C. M., A'Hearn M., 2013, Icarus, 222, 808
Davidsson B. et al., 2015, DPS meeting 47, Abstract 413. p. 15
Davis D. R., Farinella P., 1997, Icarus, 125, 50
Delbo M. et al., 2014, Nature, 508, 233
Eberhardt E., Stimpson B., Stead D., 1999, Rock Mech. Rock Eng., 32, 81
El Maarry M. R. et al., 2015, Geophys. Res. Lett., 42, 5170
Groussin O. et al., 2015, A&A, 583, A32
Gundlach B., Blum J., Keller H. U., Skorov Y. V., 2015, A&A, 583, A12
Hilchenbach M. et al., 2016, ApJ, 816, L32
Ivanova O. V., Neslušan L., Svoren J., Seman Krišandová Z., 2015, Icarus, 254, 92
Johansen A. et al., 2007, Nature, 448, 1022

Johansen A., Youdin A., Mac Low M.-M., 2009, ApJ, 704, L75
Jorda L. et al., 2016, Icarus, in press
Keller H. U. et al., 2007, Space Sci. Rev., 128, 433
Kenyon S. J., Bromley B. C., 2004, AJ, 128, 1916
Kretke K. A., Levison H. F., 2015, Icarus, 262, 9
La Forgia F. et al., 2015, A&A, 583, A41
Lamy P. et al., 2015, EPSC meeting, Abstract 783
Lee J-C. et al., 2016, LPSC meeting, Abstract 1727
Lucchetti A. et al., 2016, A&A, 585, L1
Massironi M. et al., 2015, Nature, 526, 402
Matsumura S. et al., 2014, MNRAS, 443, 3368
Michikami T. et al., 2008, Earth Planet. Space, 60, 13
Morbidelli A., Rickman H., 2015, A&A, 583, A43
Mottola S. et al., 2015, Science, 349, 6247
Nyquist H., 1928, Trans. Am. Inst. Elect. Eng., 47, 617
Pajola M. et al., 2015, A&A, 583, A37
Pajola M. et al., 2016, A&A, 585, A85
Preusker F. et al., 2015, A&A, 583, A33
Pommerol A. et al., 2015, A&A, 583, A25
Remetean E. et al., 2016, Acta Astronaut., in press
Rotundi A. et al., 2015, Science, 347, aaa3905
Rubin M. et al., 2015, Science, 348, 232
Spohn T. et al., 2015, 349, 6247
Sierks H. et al., 2015, Science, 347, aaa1044
Tancredi G., Roland S., Bruzzone S., 2015, Icarus, 247, 279
Thomas P. C. et al., 2007, Icarus 187, 4
Thomas N. et al., 2015, Science, 347, 440
Vincent J.-B. et al., 2015a, PSS, 107, 53
Vincent J.-B. et al., 2015b, Nature, 523, 63
Vincent J.-B. et al., 2016, A&A, 587, A14
Wahlberg Jansson K., Johansen A., 2014, A&A, 570, A47
Weidenschilling S. J., 1997, Icarus, 127, 290
Youdin A. N., Goodman J., 2005, ApJ, 620, 459

This paper has been typeset from a TEX/LATEX file prepared by the author.